Image Denoising via Group Sparse Eigenvectors of Graph Laplacian

Yibin Tang*, Ying Chen†, Ning Xu*, Aimin Jiang*, Lin Zhou†
*College of IOT Engineering, Hohai University, Changzhou, China
†School of Information Science and Engineering, Southeast University, Nanjing, China

Abstract—**In this paper, a group sparse model using Eigenvectors of the Graph Laplacian (EGL) is proposed for image denoising. Unlike the heuristic setting for each image and for each noise deviation in the traditional denoising method via the EGL, in our group-sparse-based method, the used eigenvectors are adaptively selected with the error control. Sequentially, a modified group orthogonal matching pursuit algorithm is developed to efficiently solve the optimal problem in this group sparse model. The experiments show that our method can achieve a better performance than some well-developed denoising methods, especially in the noise of large deviations and in the SSIM measure.**

I. Introduction

In the past decades, a number of methods have been well developed to deal with the image denoising problem [1]. However, with the advances of sparse signal representation, more methods are presented to solve this problem based on the sparse assumption, and achieve the better denoising performances compared with the traditional methods. Sparse representation is devoted to represent the signal as a linear combination of a small number of atoms from an over-complete dictionary. Early denoising methods via sparse representation, such as K-means Singular Value Decomposition (K-SVD) method [2], usually treat the denoising problem as a pure mathematical problem. In these methods, patches are separately taken into account with the neglect of the relationship with others. Later, numerous improved methods are developed to exploit such relationship, and often model the connection among sparse coefficients. For example, a nonlocally centralized sparse representation method [3] is presented to centralize the sparse coefficients into various categories, and achieves a comparable result with the well-known Block-Matching and 3D filtering (BM3D) method [4].

As for group sparse representation, it assumes that the signal can be approximated by some sub-dictionaries with grouped atoms. More specifically, the corresponding components of the signal projected on each atom group are likely to be either all zeros or all non-zeros. Contributing to this attribute, group sparse representation is widely used in various applications, such as image recognition, segment and annotation [5-7], where image features can be efficiently categorized by the sparse coefficients on these grouped atoms. Unfortunately, there are seldom reports for image denoising via group sparse representation. Since the group constraint is a somewhat strong constraint for the accurate signal representation, clean images cannot be sufficiently restored from the noisy ones, especially in noise of small deviations.

On the other hand, graph theory has been well employed in a variety of image applications in recent decades. As for image denoising, the reports also show that the denoising performance can be improved combined with the graph theory. For example, a graph regularized sparse approximation method [8] is proposed to perform a manifold embedding on sparse coefficients, in which the graph Laplacian matrix is viewed as a useful tool to exploit the geometrical structures for image patches. Very recently, a robust graph-Laplacian-based image denoising is presented with the optimal edge weights of the graph to cope with the noise [9]. Unlike the direct utilization of the graph Laplacian, a denoising method with Eigenvectors of the Graph Laplacian (EGL) is currently developed [10]. In this literature, the eigenvectors of the graph Laplacian of patches do not only represent the global features of images, but also are used as a set of basis functions to reconstruct images. Moreover, to achieve a better denoising performance, only a part of the eigenvectors is incorporated in the EGL, where the number of the used eigenvectors is fluctuated for various images and for noise of various deviations. In other words, the appropriate eigenvector number should be trivially tested for each image and noise of each deviation. In practice, it is somewhat less effective, since no clean images are given as a metric for the quality assessment of denoised images.

Motivated by the recent progress, we propose a denoising method, called as Group-Sparse-based EGL (GS-EGL), to incorporate the group sparse representation to image denoising with eigenvectors of the graph Laplacian. The major contribution of our work is threefold. 1) A group sparse model is introduced into the traditional EGL method, where the denoised image is restored with the grouped sparse coefficients in the subspace spanned by the eigenvectors. 2) An error control strategy is also employed to constrain the denoised images in an acceptable scale with the noisy ones. Here, the eigenvectors are adaptively selected from the proposed group sparse model with this error control. 3) A modified group orthogonal matching pursuit algorithm is presented to efficiently solve the optimal problem in our group sparse model with the consideration of the reliability of the eigenvectors. The experiments show that the proposed method can achieve

978-0-9928-6265-7/16/$31.00 ©2016 IEEE

a better performance than some well-developed denoising methods, especially in noise of large deviations.

II. Related Work

A. Group sparse model

In general, sparse representation can be classified in two tasks, i.e., dictionary learning and sparse approximation. The target of dictionary learning is to search an optimal signal space to support the attribution of a sparse vector under a certain measure. Meanwhile, sparse approximation is dedicated to find a sparse solution on the given dictionary. Here, we pay more attention on the sparse approximation problem. Thus, given a measurement data matrix $\boldsymbol{Y} = [\boldsymbol{y}_1\ \boldsymbol{y}_2\ ...\ \boldsymbol{y}_N]$, the basic sparse representation problem with the residual error constraint is expressed as

$$\tilde{\boldsymbol{x}}_i = \arg\min_{\boldsymbol{x}_i} \|\boldsymbol{x}_i\|_0 \ s.t. \ \|\boldsymbol{y}_i - \boldsymbol{D}\boldsymbol{x}_i\|_2^2 \leq \varepsilon, \tag{1}$$

where $\|.\|_0$ is the l_0-norm, $\boldsymbol{D} = [\boldsymbol{d}_1\ \boldsymbol{d}_2\ ...\ \boldsymbol{d}_K]$ is the dictionary with the atoms $\{\boldsymbol{d}_k\}$, $\boldsymbol{X} = [\boldsymbol{x}_1\ \boldsymbol{x}_2\ ...\ \boldsymbol{x}_N]$ is the coefficient matrix with the sparse coefficients $\{\boldsymbol{x}_i\}$, ε is a threshold for the residual error control. In image denoising, each $\boldsymbol{y}_i$ represents a noisy image patch, $\boldsymbol{Y}$ is the corresponding noisy patch matrix, and N is the number of the total patches.

For the group sparse representation, we just introduce the model in a matrix form [5] as

$$\tilde{\boldsymbol{X}} = \arg\min_{\boldsymbol{X}} \|\boldsymbol{X}\|_{2,0} \ s.t. \ \|\boldsymbol{Y} - \boldsymbol{D}\boldsymbol{X}\|_F^2 \leq \varepsilon, \tag{2}$$

where $\|.\|_F$ is the Frobenius norm, $\|\boldsymbol{X}\|_{2,0} = \sum_{i=1}^{K} \mathcal{I}(\|\boldsymbol{l}_i\|_2)$, $\boldsymbol{l}_i^T$ is the ith row vector of $\boldsymbol{X}$, $\mathcal{I}(.)$ is an indicator function defined as

$$\mathcal{I}(\|\boldsymbol{l}_i\|_2) = \begin{cases} 1, & if\ \|\boldsymbol{l}_i\|_2 > 0 \\ 0, & otherwise. \end{cases} \tag{3}$$

To tackle this group sparse problem, though a number of effective algorithms are developed in different forms, in this paper, Group Orthogonal Matching Pursuit (GOMP) method [11] is preferred for its high computation efficiency. In the GOMP, the optimal matrix $\tilde{\boldsymbol{X}}$ is achieved by the greedy strategy, where in each iteration $\boldsymbol{D}\tilde{\boldsymbol{X}}$ is approximated to the target data $\boldsymbol{Y}$ with the minimal residual error.

B. Image denoising via EGL

As for the EGL method, the basic idea is to estimate clean patches from the noisy ones on a set of the eigenvectors of the graph Laplacian. More specifically, a normalized Laplacian matrix $\boldsymbol{L}$ is firstly obtained as

$$\boldsymbol{L} = \boldsymbol{I} - \boldsymbol{B}^{-1/2}\boldsymbol{W}\boldsymbol{B}^{-1/2}, \tag{4}$$

where $\boldsymbol{I}$ is an identity matrix, $\boldsymbol{W}$ is a weight matrix for the k-nearest neighbor graph of noisy patches, $\boldsymbol{B}$ is a diagonal matrix and its diagonal entries are the row sums of $\boldsymbol{W}$. Due to the Laplacian matrix $\boldsymbol{L}$ is symmetric and positive semi-definite, its eigenvalues can be expressed as $\{\lambda_i\}_{i=1}^N$, which is lined in an ascending order with the first eigenvalue $\lambda_1 = 0$. And the corresponding eigenvectors are described as $\{\boldsymbol{u}_i\}_{i=1}^N$.

To deal with image denoising, the denoised patch matrix $\tilde{\boldsymbol{Y}}$ is represented as

$$\tilde{\boldsymbol{Y}} = \boldsymbol{Y}\boldsymbol{U}_M\boldsymbol{U}_M^T, \tag{5}$$

where $\boldsymbol{U}_M = [\boldsymbol{u}_1\ \boldsymbol{u}_2\ ...\ \boldsymbol{u}_M]$ is a basis matrix with the first M low-order eigenvectors.

In practice, the EGL employs an iterative procedure to deal with the noisy image, which is divided into two major stages. In the first stage, a rough image as a lowpass version of the clean image is estimated by using a very small number of the eigenvectors of the graph Laplacian from the noisy image. Note that, these selected eigenvectors are insensitive to images and noise deviations, whose target is only to enhance the image intrinsic structures. Sequentially, an intermediate image is constructed with a weighted average of the noisy and rough images, and used as a guided image in the following denoising. In the second stage, the denoised image is restored from this guided image by the corresponding eigenvectors. Unlike in the first stage, the appropriate number of the eigenvectors here is carefully set in order to achieve a better denoising performance, which is fluctuated for various images and for noise of various deviations.

III. Proposed Algorithm

A. Group sparse model for EGL

To introduce group sparse model into the EGL, we first show (5) in its group sparse form. More conveniently, we transform (5) into the formula as

$$\tilde{\boldsymbol{G}} = \boldsymbol{U}_M\boldsymbol{U}_M^T\boldsymbol{G}, \tag{6}$$

where $\boldsymbol{G}$ and $\tilde{\boldsymbol{G}}$ are the transpose matrices of $\boldsymbol{Y}$ and $\tilde{\boldsymbol{Y}}$, respectively. In (6), each column of $\boldsymbol{G}$ is projected into a subspace spanned by the vectors of $\boldsymbol{U}_M$, and then the denoised matrix $\tilde{\boldsymbol{G}}$ is achieved on such subspace. We further rewrite (6) in the full space of $\boldsymbol{U} = [\boldsymbol{u}_1\ \boldsymbol{u}_2\ ...\ \boldsymbol{u}_N]$ as

$$\begin{cases} \tilde{\boldsymbol{G}} = \boldsymbol{U}\boldsymbol{X} \\ \boldsymbol{X} = \begin{pmatrix} \boldsymbol{U}_M^T\boldsymbol{G} \\ \boldsymbol{0} \end{pmatrix}. \end{cases} \tag{7}$$

In (7), since only the first M row vectors of the coefficient matrix $\boldsymbol{X}$ are non-zeros, it can be viewed as a special form with the group sparse structure. As the extension of (7), we propose a basic group sparse model to achieve the denoised matrix $\tilde{\boldsymbol{G}}$ as

$$\begin{cases} \tilde{\boldsymbol{G}} = \boldsymbol{U}\tilde{\boldsymbol{X}} \\ \tilde{\boldsymbol{X}} = \arg\min_{\boldsymbol{X}} \|\boldsymbol{X}\|_{2,0} \ s.t. \ \|\boldsymbol{G} - \boldsymbol{U}\boldsymbol{X}\|_F^2 \leq \varepsilon. \end{cases} \tag{8}$$

Compared with (7), there are two significant differences in (8). First, the residual error control is given to constrain the denoised matrix $\tilde{\boldsymbol{G}}$ in the acceptable scale with the noisy one $\boldsymbol{G}$. Second, the eigenvectors can be more flexibly selected with an appropriate number $\|\boldsymbol{X}\|_{2,0}$ instead of the fixed first M eigenvectors in the EGL. Note that, though the matrix $\boldsymbol{U}$ should be an orthogonal matrix mathematically as the result of the matrix singular value decomposition, in practice, the orthogonal attribute cannot be fully guaranteed, since some fast computation algorithms [10] are used to achieve the approximated eigenvectors. Therefore, it is more reasonable to utilize our group sparse model to achieve the better denoised matrix $\tilde{\boldsymbol{G}}$.

In details, we only modify the EGL method in its second stage. Thus, several parameters in the first stage of the EGL, i.e., the intermediate image patch matrix $\hat{\boldsymbol{Y}}$, and its corresponding transpose $\hat{\boldsymbol{G}}$ and eigenvector matrix $\hat{\boldsymbol{U}}$, are already given. Thus, we build a more exquisite group sparse model as

$$\begin{cases} \tilde{\boldsymbol{G}} = \hat{\boldsymbol{U}}\tilde{\boldsymbol{X}} \\ \tilde{\boldsymbol{X}} = \arg\min_{\boldsymbol{X}} \|\boldsymbol{X}\|_{2,0} + \alpha\|\hat{\boldsymbol{G}} - \hat{\boldsymbol{U}}\boldsymbol{X}\|_F \\ s.t.\ \|\boldsymbol{G} - \hat{\boldsymbol{U}}\boldsymbol{X}\|_F^2 \le \varepsilon, \end{cases} \tag{9}$$

where α is a weight coefficient. As aforementioned in the EGL, $\hat{\boldsymbol{Y}}$ is used as a guided matrix for the denoised patch matrix $\tilde{\boldsymbol{Y}}$ in order to further improve the denoising performance. Here, in the regularization term of (9), the corresponding $\hat{\boldsymbol{G}}$ is also used for this purpose, which provides a guided target for $\boldsymbol{X}$ to achieve a better $\tilde{\boldsymbol{G}}$. Finally, $\tilde{\boldsymbol{Y}}$ can be achieved with the transpose of $\tilde{\boldsymbol{G}}$.

B. Solution for proposed group sparse model

To solve the group sparse problem in (9), a modified GOMP algorithm is proposed as shown in *Algorithm 1*. Since we set $\hat{\boldsymbol{G}}$ as a guided matrix, the regularization term $\|\hat{\boldsymbol{G}} - \hat{\boldsymbol{U}}\boldsymbol{X}\|_F$ should be greedily minimized in each iteration of our modified GOMP, where it replaces the minimization strategy for the residual error by the traditional GOMP in (8). More details of the parameters in the modified GOMP are given as follows. S is an index set, $\boldsymbol{R}$ is a residual error matrix with respect to $\hat{\boldsymbol{G}}$, and $\boldsymbol{w}$ is a weight vector with its entries $w_i = i$. Moreover, $\boldsymbol{U}_S$ is a sampled version of $\hat{\boldsymbol{U}}$, where the vectors of $\hat{\boldsymbol{G}}$ indexed by S are reserved and other vectors are set to zeros. $\boldsymbol{U}'$ is a matrix, in which all other vectors are orthogonal to a selected vector. $\boldsymbol{X}'$ is a coefficient matrix of $\boldsymbol{R}$ on $\boldsymbol{U}'$.

In the modified GOMP, the procedure can be summarized into two major stages. In the first stage, it focuses to detect the group sparse location, where the index set S is incorporated to record the used rows in $\boldsymbol{X}$. Sequentially, the corresponding sparse coefficients on these locations are calculated in the second stage. It is worth mentioning that, since the noise tends to disturb the high-order eigenvectors than those low-order ones [10], in the first stage, we use the weight vector $\boldsymbol{w}$ to measure the fidelity of each eigenvector. As a result, the low-order eigenvectors have more opportunity to be selected compared with the high-order ones in our algorithm. Consequentially, the denoised matrix $\tilde{\boldsymbol{G}}$ can be more reliably restored.

Here, the solution feasibility of (9) is also considered. Since $\hat{\boldsymbol{G}}$ can be fully represented in the space spanned by the vectors of $\hat{\boldsymbol{U}}$, a feasible solution of $\boldsymbol{X}$ can be always achieved with $\hat{\boldsymbol{G}} = \hat{\boldsymbol{U}}\boldsymbol{X}$, if $\|\boldsymbol{G} - \hat{\boldsymbol{G}}\|_F^2 \le \varepsilon$. In practice, this condition can be almost met with the well setting in the generation of the intermediate image for the EGL. Consequentially, the solution of (9) can be guaranteed.

Algorithm 1: Modified GOMP

Input: transpose matrices $\boldsymbol{G}$ and $\hat{\boldsymbol{G}}$, eigenvector matrix $\hat{\boldsymbol{U}}$, weight vector $\boldsymbol{w}$, index set S, residual error threshold ε.
Output: optimal sparse coefficient matrix $\tilde{\boldsymbol{X}}$ and transpose matrix $\tilde{\boldsymbol{G}}$.
1. Init: $\boldsymbol{X} = \boldsymbol{0}$, $\boldsymbol{R} = \hat{\boldsymbol{G}}$, $\boldsymbol{U}' = \hat{\boldsymbol{U}}$, $\boldsymbol{U}_S = \boldsymbol{0}$, $S = \varnothing$
2. **while** $\|\boldsymbol{G} - \hat{\boldsymbol{U}}\boldsymbol{X}\|_F^2 > \varepsilon$
   Stage 1: group sparse location detection
3. $\boldsymbol{X}' = (\boldsymbol{U}')^T\boldsymbol{R}$.
4. $k = \arg\min_i \boldsymbol{w}_i\|\boldsymbol{R} - \boldsymbol{u}_i'\boldsymbol{l}_i^T\|_F^2$, $\boldsymbol{u}_i'$ and $\boldsymbol{l}_i^T$ are the ith vector of $\boldsymbol{U}'$ and row vector of $\boldsymbol{X}'$ respectively.
5. $S = S \cup \{k\}$.
6. Update $\boldsymbol{U}'$, and let all vectors $\boldsymbol{u}_i'$ with $\langle \boldsymbol{u}_{i\neq k}', \boldsymbol{u}_k' \rangle = 0$.
7. Set $\boldsymbol{u}_k' = \boldsymbol{0}$.
   Stage 2: group sparse coefficient calculation
8. Update $\boldsymbol{U}_S$ with the vectors of $\hat{\boldsymbol{U}}$ indexed by S.
9. $\boldsymbol{X} = \boldsymbol{U}_S^{-1}\hat{\boldsymbol{U}}$.
10. $\boldsymbol{R} = \hat{\boldsymbol{G}} - \hat{\boldsymbol{U}}\boldsymbol{X}$.
11. **end**
12. $\tilde{\boldsymbol{X}} = \boldsymbol{X}$, $\tilde{\boldsymbol{G}} = \hat{\boldsymbol{U}}\tilde{\boldsymbol{X}}$.

Fig. 1. Clean images. From left to right, images are named as *Barbara*, *Lena*, *Mandrill*, *Boat* and *Clown*, respectively.

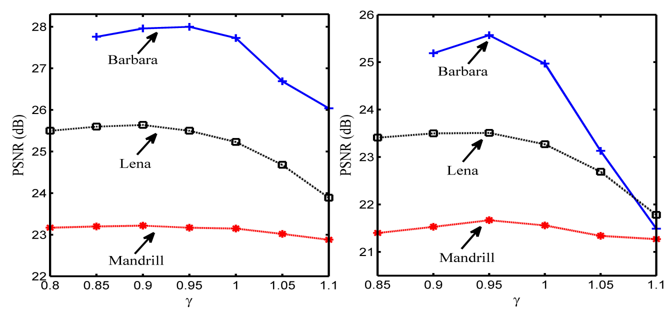

Fig. 2. Denoising performances with weight coefficient γ. The left and right figures are in noise of the deviations $\sigma = 40$ and $\sigma = 60$, respectively.

IV. Simulations

In our test, a set of images are used with a size of 128×128 pixels shown in Fig. 1. Meanwhile, the proposed GS-EGL method is compared with the other three well-developed methods, i.e., the K-SVD, BM3D and Expected Patch Log Likelihood (EPLL) [12] methods. Noisy images are obtained by adding Gaussian noise with various levels. In our GS-EGL, all parameters are used as the same as those in the traditional EGL. Moreover, since the high-order eigenvectors are less reliable than the low-order ones, a part of eigenvectors are calculated for the GS-EGL. For example, the first 1500, 1000 and 600 eigenvectors of the intermediate image are initially calculated for noises of the deviations $\sigma = 20, 40, 60$, respectively.

To achieve the better residual error threshold in various noise deviations, a set of threshold values are tested for different images. The threshold is set as $\varepsilon = \gamma Nb\sigma^2$, where γ

Fig. 3. Denoising performance comparisons with the noise deviation $\sigma = 40$. From left to right for each line, denoised images are obtained via the K-SVD, BM3D, EPLL and GS-EGL, respectively.

Fig. 4. Denoising performance comparisons with the noise deviation $\sigma = 60$. From left to right for each line, denoised images are obtained via the K-SVD, BM3D, EPLL and GS-EGL, respectively.

is a weight coefficient, b is the patch size of 3×3. Thus, the denoised performances with the parameter γ are given in Fig. 2. It shows that, the better denoising performances can be achieved with $\gamma = 0.9$ and 0.95 for noise of the deviations $\sigma = 40$ and 60, respectively. When γ is small, the performance is worse. It is because, with the error constraint of the over tight threshold, the denoised images tend to be close to the intermediate images. Meanwhile, with the larger γ, the performance of restored images is also deteriorated. In this situation, the threshold is too loose to efficiently provide the valid information of noise for denoising. Moreover, in this experiment, it is proven that the initial eigenvector numbers of the intermediate image are enough for the proposed GS-EGL.

The denoised image comparison between the GS-EGL and the other three methods in the noise deviation $\sigma = 40$ is shown in Fig. 3. The performance of the K-SVD is the worst with an amount of details and textures lost. It is because the features contained in the atoms are obscured by noise, for its dictionary is directly trained from the noisy images. The BM3D outperforms the K-SVD. However, the BM3D shows the limited ability to rebuild the noise-like details. As shown in Mandrill, more details in the fur areas are lost, due to the joint filtering approach used in the BM3D here can be viewed as a lowpass filter to some extent. Therefore, these fur areas, which contain more information in the high frequency domain, inevitably tend to be over smoothed with the large distortion. As for the EPLL, it can better deal with the details in Mandrill. It benefits from the Gaussian Mixture Model (GMM) which estimates the patch prior information for denoising. But it is less efficient for the texture restoration in Barbara, since the EPLL only focuses on the single patch reconstruction as a local denoising method. In the GS-EGL, both the details and textures are restored. These details and textures are all viewed as the structures and can be well described via the eigenvectors of the graph Laplacian of images as global features. More importantly, to achieve these results, the GS-EGL adaptively chooses these eigenvectors by the residual error threshold. It means that, unlike the heuristic setting in the traditional EGL, the eigenvector selection problem is well solved in our method.

The denoised images with the noise deviation $\sigma = 60$ are shown in Fig. 4. The K-SVD still performs the worst. The BM3D achieves a more acceptable result. However, it still tolerates the smoothing problem just as in Fig. 3. The denoising performance of the EPLL becomes even worse than the BM3D. Now, numerous classification errors exist in the EPLL, that is, the wrong Gaussian model is used for the corresponding patch with the serious noise perturbation. As for the GS-EGL, compared with the BM3D, the details and textures can still be restored, due to the structures are robustly indicated in the eigenvectors. However, there exist some stain artifacts in the flat areas, e.g., the cheek of Lena. In this case, the noise is identified as structures of the image and then introduced into the eigenvectors. As a result, the false structures are emphasized in the denoised images. Note that, these denoised results are also only achieved by the residual error threshold without any prior on the eigenvector selection.

To estimate the GS-EGL in the noise of various levels, the statistical results are given with both the PSNR and SSIM measures in Table I. It shows that, the K-SVD performs the worst. The BM3D can well deal with the noisy images in various noise levels, for its joint filtering approach. As for the EPLL, it achieves the better denoising performance than the BM3D in noise of the small deviation, e.g., $\sigma = 20$, since the GMM is used for the patch prior. However, it deteriorates with the noise deviation increasing, due to the aforementioned classification errors for Gaussian models. In the GS-EGL, it achieves the best denoising performance in noise of the large deviations, such as $\sigma = 40$ and 60, especially in the SSIM measure. It benefits from two aspects, that is, the global structure exploitation by the eigenvectors and the residual error control guided with the intermediate image. However, it also shows that, in the small noise deviation, $\sigma = 20$, the

TABLE I
PSNR (dB) AND SSIM RESULTS BY DIFFERENT DENOISING METHODS.

σ		20	40	60
Barbara	K-SVD	30.97 / 0.9847	26.33 / 0.7668	24.42 / 0.6721
	BM3D	**31.42 / 0.9119**	27.00 / 0.8037	25.41 / 0.7336
	EPLL	30.46 / 0.8956	26.52 / 0.7839	24.71 / 0.6990
	GS-EGL	30.62 / 0.8804	**27.96 / 0.9083**	**25.57 / 0.7521**
Boat	K-SVD	29.47 / 0.8771	25.25 / 0.7433	23.00 / 0.6316
	BM3D	29.60 / **0.8894**	25.88 / 0.7857	24.08 / 0.7064
	EPLL	**29.66** / 0.8873	26.05 / 0.7912	24.14 / 0.7110
	GS-EGL	28.77 / 0.8656	**26.08 / 0.7912**	**24.19 / 0.7208**
Clown	K-SVD	28.52 / 0.8649	24.66 / 0.7117	22.45 / 0.6084
	BM3D	28.94 / 0.8895	24.84 / 0.7721	22.80 / 0.6842
	EPLL	**29.07 / 0.8925**	25.26 / 0.7575	**23.30** / 0.6547
	GS-EGL	28.18 / 0.8667	**25.29 / 0.7836**	23.19 / **0.6872**
Mandrill	K-SVD	26.03 / 0.7929	22.93 / 0.5687	21.57 / 0.4357
	BM3D	26.12 / 0.8070	22.89 / 0.5727	**21.89** / 0.4627
	EPLL	**26.40 / 0.8269**	23.00 / 0.5947	21.71 / 0.4571
	GS-EGL	25.78 / 0.7973	**23.22 / 0.6556**	21.67 / **0.4970**
Lena	K-SVD	28.69 / 0.8472	24.90 / 0.6926	22.99 / 0.5899
	BM3D	29.04 / 0.8653	25.28 / 0.7221	**23.69 / 0.6415**
	EPLL	**29.05 / 0.8654**	25.34 / 0.7372	23.51 / 0.6382
	GS-EGL	28.05 / 0.8176	**25.64 / 0.7373**	23.51 / 0.6237

performance of the GS-EGL is somewhat terrible. Here, the intermediate image not only is used as a guided image to restore the final denoised image, but also can be viewed as a structure-emphasized version of the noisy image. Therefore, the distortion is inevitably introduced. Though this distortion is benefit to restore the denoised images in the large noise deviations, it is still harmful to separate clean images from the noisy ones in the small noise deviation.

V. Conclusion

The GS-EGL method is presented to incorporate the group sparse model to image denoising with eigenvectors of the graph Laplacian. With the error control to reconstruct the denoised images in the acceptable scale of the noisy ones, the used eigenvectors can be adaptively selected from the proposed group sparse model, where the heuristic setting in the traditional EGL is avoided for various images and noise deviations. The experiments show that, our method can achieve the better performance than some well-developed denoising methods, especially in noise of the large deviations. Note that, the computation complexity of the GS-EGL is less discussed. In actually, the computation of the proposed modified GOMP algorithm is quite efficient. However, the GS-EGL spends an enormous number of time to obtain the eigenvectors just as the traditional EGL. Therefore, in the future work, we will focus to reduce the computation complexity for these eigenvectors.

Acknowledgment

This work is supported by National Nature Science Foundation of China under grants 61401148, 61471157, 61501169 and 61571106, the Natural Science Foundation of Jiangsu Province, China under grants BK20130238 and BK20141159, the Fundamental Research Funds for the Central Universities under grant 2016B08814.

References

[1] A. Buades, B. Coll, J. M. Morel, A review of image denoising algorithms, with a new one, *Multiscale Model. Simul.*, vol. 4, no. 2, pp. 490-530, 2005.

[2] M. Aharon, M. Elad, A. Bruckstein, K-SVD: An algorithm for designing overcomplete dictionaries for sparse representation, *IEEE Trans. Signal Process.*, vol. 54, no. 11, pp. 4311-4322, 2006.

[3] W. Dong, L. Zhang, G. Shi, X. Li, Nonlocally centralized sparse representation for image restoration, *IEEE Trans. Image Process.*, vol. 22, no. 4, 1620-1630, 2013.

[4] K. Dabov, A. Foi, V. Katkovnik, K. Egiazarian, Image denoising by sparse 3D transform-domain collaborative filtering, *IEEE Trans. Image Process.*, vol. 16, no. 8, pp. 2080-2095, 2007.

[5] Y. Sun, Q. Liu, J. Tang, D. Tao, Learning discriminative dictionary for group sparse representation, *IEEE Trans. Image Process.*, vol. 23, no. 9, pp. 3816-3828, 2014.

[6] X. Lu, X. Li, Group sparse reconstruction for image segmentation, *Neurocomputing*, vol. 136, pp. 41-48, 2014.

[7] S. Gao, L. Chia, I. Tsang, Z. Ren, Concurrent single-label image classification and annotation via efficient multi-layer group sparse coding, *IEEE Trans. on Multimedia*, vol. 16, no. 3, pp. 762-771, 2014.

[8] Y. Tang, Y. Shen, A. Jiang, et al., Image denoising via graph regularized K-SVD, in *IEEE Int. Symp. on Circuits and Systems*, pp. 2820-2823, 2013.

[9] J. Pang, G. Cheung, A. Ortega, O. Au, Optimal graph Laplacian regularization for natural image denoising, in *IEEE Int. Conf. on Acoustics, Speech and Signal Processing*, 2294-2298, 2015.

[10] F. G. Meyer, X. Shen, Perturbation of the eigenvectors of the graph Laplacian: Application to image denoising, *Appl. Comput. Harmonic Anal.*, vol. 36, no. 2, 326-334, 2014.

[11] A. Majumdar, R. Ward, Fast group sparse classification, *Canadian Journal of Electrical and Computer Engineering*, vol. 34, no.4, 136-144, 2009.

[12] G. Yu, G. Sapiro, S. Mallat, Solving inverse problems with piecewise linear estimators: From Guassian mixture models to structured sparsity, *IEEE Trans. Image Process.*, vol. 21, no. 5, pp. 2481-2499, 2012.